

## Original Article

# Correlation between signal changes on MRI sequences and cartilage histopathologic variation after cartilage impact injury in the knee joint: an animal study

Hongliang Gao<sup>1</sup>, Yongli Wang<sup>1</sup>, Xinhua Zhou<sup>1</sup>, Meng Wu<sup>1</sup>, Xinfeng Mao<sup>2</sup>, Wei Fang<sup>3</sup>, Xiongfeng Li<sup>1</sup>, Jianyou Li<sup>1</sup>

Departments of <sup>1</sup>Orthopedics, <sup>2</sup>Radiology, <sup>3</sup>Pathology, Huzhou Central Hospital, Huzhou City, Zhejiang Province, P.R. China

Received February 28, 2018; Accepted April 7, 2018; Epub June 15, 2018; Published June 30, 2018

**Abstract:** Objective: Our aim was to explore correlation between changes in signals on diverse MRI sequences and histopathologic variation in cartilage following cartilage impact injuries of knee joints in rabbits. Methods: A total of 120 New Zealand white rabbits were included for constructing rabbit models of cartilage impact injuries in knee joints by simulating the mechanisms of cartilage impact injuries of human knee joints and impacting with self-made impactors. The constructed rabbit models were assigned to a high-intensity group (impact from a height of 60 cm), medium-intensity group (impact from a height of 45 cm), and low-intensity group (impact from a height of 35 cm), based on impact intensity. Magnetic resonance imaging (MRI) was conducted for examining bilateral knee joints of the lower extremities in animals at 6 hours, 2 weeks, and 4 weeks after modeling and signal-to-noise ratio (SNR) was calculated. After every MRI examination, specimens of injured knee joints were pooled for investigation of histopathologic variations of cartilage tissue under a light microscope. Results: Of 120 rabbit specimens, 108 were modeled successfully. All MRI findings revealed high-signal opacities after successful modeling. In the high-intensity and medium-intensity groups, significant medial soft tissue injuries of the knee joint and a small amount of intra-articular effusion were visualized. High signal changes were shown at the ends of the bone in rabbits 6 hours after modeling. In the low-intensity group, medial soft tissue injuries were milder and there was no visible intra-articular effusion in knee joints. All abovementioned symptoms were improved at 2 weeks and there were no significant differences among the three groups at 4 weeks. Among the three MRI sequences of T1WI, T2WI, and GER (gradient echo sequence), the highest SNR was detected on GER followed by T2WI. The lowest SNR was shown on T1WI. SNRs detected on all sequences decreased over time. Histopathologic detection indicated that rabbit models of the three groups were generally matched in cartilage, cortical bone, chondrocytes, and cartilage matrix at 6 hours, 2 weeks, and 4 weeks. In the high-intensity group and medium-intensity group, significant bone marrow hemorrhage and edema were noted in pathological sections at 6 hours and 2 weeks but not seen in low-intensity group. At 3 weeks, no significant improvements were observed in bone marrow hemorrhage and edema for all three groups. Conclusion: High-signal opacities for cartilage impact injuries in knee joints in rabbits were detected on the MRI sequences of T1WI, T2WI, and GER and they decreased over time after modeling. Bone marrow hemorrhage and edema were the most significant among knee joint injuries on the GER sequence.

**Keywords:** Knee joint, MRI, animal model, cartilage tissue, pathology

## Introduction

According to statistics provided by Graham et al., a traffic accident takes place every 10 seconds worldwide [1]. Karimi et al. also argued that 62.8% of the accidents result in death and casualties. Joint injury and fractures induced by high-energy trauma are most common [2]. Kindig et al. reported that, among patients that

had high energy traumas after traffic accidents, more than 120,000 developed joint injuries in the United States in 2016 [3]. With an increase in the number of vehicles, the above figure is on the rise [4]. The knee joint is not only the largest joint with the most complex structure in the human body, it is also the most vulnerable joint to traffic accidents [8]. Moreover, the knee joint is the most weight-loading joint in the human

**Table 1.** MRI sequences and SNR calculation

MRI sequence	TR (ms)	TE (ms)	Slice thickness (mm)
T1WI	4000	117	3
T2WI	3000	107	3
GER	620	80	3

SNR=Bone-end signal intensity/Background noise.

body and is closely related to human activity [9, 10]. Currently, knee joint injury is the most frequently-occurred articular injury in orthopedics. Clinically, arthrography is the major imaging tool utilized for diagnosis and treatment of most knee injuries [11, 12]. However, fractures and traumas induced by non-cortical rupture or displacement of the subchondral bone in knee joints are difficult to diagnose accurately and tend to be ignored on arthrography. As a result, patients have poor response to subsequent treatment and have even aggravated injuries [13-15]. After treatment, they are prone to develop degenerative articular cartilage, resulting in traumatic arthritis. They have even become disabled because of untimely treatment or disease progression, seriously affecting the quality of life of patients [5, 6]. Correct diagnosis, visibility of the cartilage injury, accurate judgement of the severity of cartilage impact injuries, and symptomatic treatment are essential for improvement of prognosis in patients.

Currently, magnetic resonance imaging (MRI) is the most sensitive tool for diagnosis of cartilage impact injuries [7]. MRI is characterized by high contrast and multi-parameters. It visualizes injuries at the knee joint from multiple dimensions and has a high sensitivity to bone marrow hemorrhage and edema. Moreover, it can detect injuries that have been clinically occult, previously. As a result, MRI is the most common tool for detection of knee joints [16, 17]. Nevertheless, few studies have been globally focused on investigating various MRI sequences with regard to early osseous articular impact injuries and no reports have explored the correlation between MRI and histopathologic changes in cartilage tissue. Therefore, in this present study, animal models of knee cartilage impact injuries were constructed to explore the association between MRI and pathological changes in knee cartilage. Our aim was to provide a more effective and reliable reference for

clinical treatment of articular impact injuries in patients.

## Materials and methods

### Animal data

A total of 120 New Zealand white rabbits with a mean age of 6 months and weight of  $2.5 \pm 0.5$  kg were purchased from Beijing Medical Services Biotechnology, China.

### Modeling

According to a modeling method suggested by Vavalle et al., through simulating the mechanisms of cartilage impact injuries in human knee joints, rabbit models of articular cartilage impact injuries were constructed by vertically impacting the right knee articular cartilage of rabbits along the guide rod from respective heights of 60 cm, 45 cm, and 35 cm with a 0.400-kg hammer (10 cm long, 5 cm wide, and 10 cm high) on a self-made impactor. At the end of the impacts, presence of joint injury but no fracture on radiography was considered as successful modeling.

### Experimental procedures

Successful rabbit models were randomly assigned to the high-intensity group (impact from a height of 60 cm), medium-intensity group (impact from a height of 45 cm), and low-intensity group (impact from a height of 35 cm) in terms of impact intensity. MRI was performed to examine bilateral knee joints of lower extremities in rabbits using a 1.5T MR scanner (Siemens, Germany) at 6 hours, 2 weeks, and 4 weeks after impact. MRI sequences are listed in **Table 1** and the signal-noise ratio (SNR) was calculated. Findings of all MRIs were evaluated in a double-blind manner by 3 senior radiologists from our hospital. After each MRI examination, 15 rabbits (5 in each group) were sacrificed, from which knee joint specimens were extracted. Extracted specimens were fixed in 10% formaldehyde solution followed by observation of the pathological sections (bone marrow hemorrhage, edema, and trabecular structure) under a light microscope.

### Statistical analysis

Data were analyzed with use of SPSS statistics software, version 22.0. Count data are

## Signal changes on MRI sequences and cartilage histopathologic variation

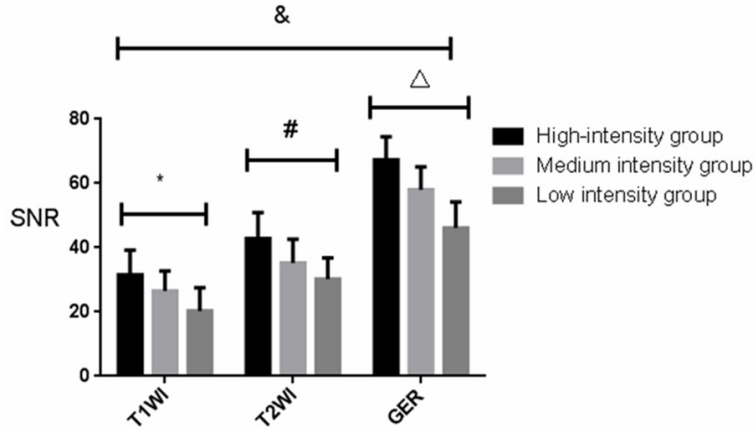


**Figure 1.** SNRs on all three sequences at 6 hours after modeling. The SNRs of the high-intensity group, medium-intensity group, and low-intensity group on T1WI were  $31.51 \pm 7.69$ ,  $26.58 \pm 6.09$ , and  $20.27 \pm 7.31$ , respectively; the corresponding SNRs on T2WI were  $42.84 \pm 8.07$ ,  $35.24 \pm 7.41$ , and  $30.21 \pm 6.62$ , respectively; the corresponding SNRs on GER were  $67.28 \pm 7.29$ ,  $58.04 \pm 7.05$ , and  $46.17 \pm 8.05$ , respectively. \* $P < 0.05$ , comparisons of the SNRs on T1WI among the three groups, with the highest SNR in the high-intensity group; # $P < 0.05$ , comparisons of the SNRs on T2WI among the three groups, with the highest SNR in the high-intensity group; <sup>a</sup> $P < 0.05$ , comparisons of the SNRs in GER among the three groups, with the highest SNR in the high-intensity group; <sup>&</sup> $P < 0.05$ , comparisons of the SNRs of the three groups on the three sequences, with the highest SNR on GER.

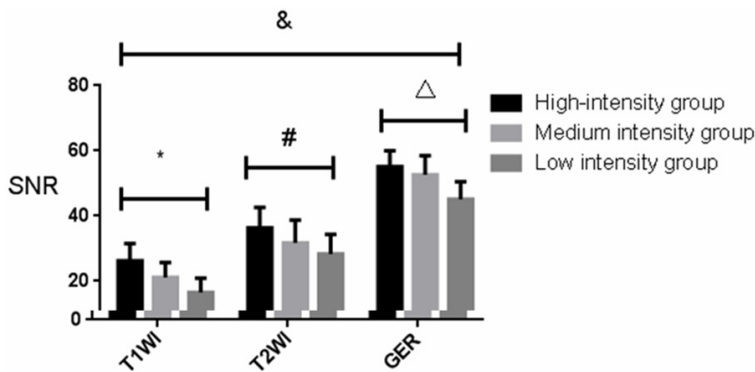


**Figure 2.** SNRs on all three sequences at 2 weeks after modeling. The SNRs of rabbits in the high-intensity group, medium-intensity group, and low-intensity group on T1WI were  $26.21 \pm 5.27$ ,  $21.18 \pm 4.56$ , and  $16.49 \pm 4.38$ , respectively; the corresponding SNRs on T2WI were  $36.36 \pm 6.25$ ,  $31.77 \pm 7.02$ , and  $28.38 \pm 6.01$ , respectively; the corresponding SNRs on GER were  $55.14 \pm 4.87$ ,  $52.66 \pm 5.94$ , and  $45.17 \pm 5.36$ , respectively. \* $P < 0.05$ , comparisons of the SNRs on T1WI among the three groups, with the highest SNR in the high-intensity group; # $P < 0.05$ , comparisons of the SNRs on T2WI among the three groups, with the highest SNR in the high-intensity group; <sup>a</sup> $P < 0.05$ , comparisons of the SNRs on GER among the three groups, with the highest SNR in the high-intensity group; <sup>&</sup> $P < 0.05$ , comparisons of the SNRs of the three groups on the three sequences, with the highest SNR on GER.

expressed as rates and between-group comparisons were made using Chi-square test and partitioning Chi-square test. Measurement

data are described as mean  $\pm$  standard deviation with one-way ANOVA and Bonferroni post hoc tests for between-group comparisons. Statistical significance for all analyses was set at  $P < 0.05$ .

## Results

### Modeling results

Of 120 rabbits, 108 models were constructed successfully with a success rate of 90%. Among successful rabbit models, 38 rabbits were in the high-intensity group, 36 in medium-intensity group, and 34 in low-intensity group.

### MRI findings 6 hours after modeling

MRI findings revealed high-signal opacities in rabbits of the three groups. Among rabbits in the high-intensity and medium-intensity groups, medial soft tissue injuries of the knee joints were significant and there was a small amount of visible intraarticular effusion with high-intensity signal changes present at the ends of the bone. In contrast, among rabbits in the low-intensity group, medial soft tissue injuries of the knee joint were milder and there was no visible intraarticular effusion. The T1 weighted images (WI) revealed that SNRs of rabbits in the high-intensity group, medium-intensity group, and low-intensity group were  $31.51 \pm 7.69$ ,  $26.58 \pm 6.09$ , and  $20.27 \pm 7.31$ , respectively, with the highest SNR in the high-intensity group ( $P = 0.001$ ). On T2WI, the corresponding SNRs were  $42.84 \pm 8.07$ ,  $35.24 \pm 7.41$ , and  $30.21 \pm 6.62$ , respectively, with the

highest SNR in high-intensity group ( $P = 0.001$ ). Corresponding SNRs in gradient echo sequence (GER) were  $67.28 \pm 7.29$ ,  $58.04 \pm 7.05$ , and

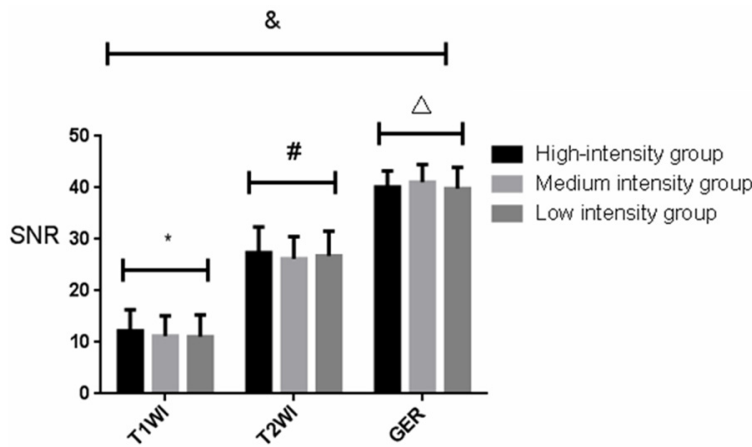


**Figure 3.** SNRs on all three sequences at 4 weeks after modeling. The SNRs of rabbits in the high-intensity group, medium-intensity group, and low-intensity group on T1WI were 12.17±4.16, 11.23±3.92, and 11.08±4.28, respectively; the corresponding SNRs on T2WI were 27.38±5.01, 26.24±4.26, and 26.77±4.81, respectively; the corresponding SNRs on GER were 40.16±3.12, 41.08±3.46, and 39.87±4.05, respectively. \*P<0.05, comparisons of the SNRs on T1WI among the three group, with the highest SNR on GER. #P<0.05, comparisons of the SNRs on T2WI among the three groups, with the highest SNR in the high-intensity group; ΔP<0.05, comparisons of the SNRs on GER among the three groups, with the highest SNR in the medium-intensity group; &P<0.05, comparisons of the SNRs of the three groups on the three sequences, with the highest SNR on GER.

46.17±8.05, respectively, with the highest SNR in high-intensity group (P=0.001). Among the three MRI sequences, SNRs of all three groups in GNR were superior to those on TIWI and T2WI (all P=0.001, **Figure 1**).

*MRI findings at 2 weeks after modeling*

MRI sequences indicated high-signal opacities of rabbits in the three groups. Compared with those at 1 hour, high-signal opacities were attenuated in medial soft tissue of the knee joint and intraarticular effusion was partly absorbed. On T1WI, SNRs of rabbits in the high-intensity group, medium-intensity group, and low-intensity group were 26.21±5.27, 21.18±4.56, 16.49±4.38, respectively, with the highest SNR in high-intensity group (P=0.001). On T2WI, corresponding SNRs were 36.36±6.25, 31.77±7.02, and 28.38±6.01, respectively, with the highest in high-intensity group (P=0.001). On GER, corresponding SNRs were 55.14±4.87, 52.66±5.94, and 45.17±5.36, respectively, with the highest in high-intensity group (P=0.001). Among the three groups, the SNR of each group on GNR was superior to TIWI and T2WI (P=0.001). However, compared to those at 6 hours, SNRs of the three groups were

reduced on all three MRI sequences (**Figure 2**).

*Findings of MRI at 4 weeks after modeling*

MRI sequences for rabbits in the three groups showed high-signal opacities. Medial soft tissue injuries of the knee joints were not significant and intraarticular effusion was completely absorbed in the three groups of rabbits. On T1WI, SNRs of rabbits in the high-intensity group, medium-intensity group, and low-intensity group were 12.17±4.16, 11.23±3.92, and 11.08±4.28, respectively, and differences were insignificant (P=0.579). On T2WI, corresponding SNRs were 27.38±5.01, 26.24±4.26, and 26.77±4.81, respectively, and differences were also insignificant (P=0.674). On GER, corresponding SNRs were 40.16

±3.12, 41.08±3.46, and 39.87±4.05, respectively, and there were no significant differences among the three groups (P=0.448). Among the three groups, the SNR of each group on GNR was superior to TIWI and T2WI (P=0.001). However, compared to those at 2 weeks, SNRs of the three groups decreased on all three MRI sequences (**Figure 3**).

*Histopathologic variations*

Rabbit models in all three groups were largely similar in cartilage, cortical bone, chondrocytes, and cartilage matrix at 6 hours, 2 weeks, and 4 weeks after modeling. At 6 hours and 2 weeks, overt bone marrow hemorrhage and edema were visible in the pathological sections of rabbits in the high-intensity and medium-intensity groups but they were invisible in rabbits of the low-intensity group. At 3 weeks, no significant improvements were observed in bone marrow hemorrhage and edema (**Table 2**).

**Discussion**

The results of our study demonstrated that there were high-signal opacities of articular impact injuries in knee joints on MRI scans.

## Signal changes on MRI sequences and cartilage histopathologic variation

**Table 2.** Histopathological profile

		High-intensity group	Medium-intensity group	Low-intensity group
6 h after modeling	Cartilage	Smooth and intact	Smooth and intact	Smooth and intact
	Cortical bone	Smooth, flat and continuous	Smooth, flat and continuous	Smooth, flat and continuous
	Chondrocyte	Normal	Normal	Normal
	Cartilage matrix	Normal	Normal	Normal
	Bone marrow hemorrhage	Evident	Evident	Invisible
	Edema	Evident	Evident	Invisible
2 w after modeling	Cartilage	Smooth and intact	Smooth and intact	Smooth and intact
	Cortical bone	Smooth, flat and continuous	Smooth, flat and continuous	Smooth, flat and continuous
	Chondrocyte	Normal	Normal	Normal
	Cartilage matrix	Normal	Normal	Normal
	Bone marrow hemorrhage	Evident	Evident	Invisible
	Bone marrow edema	Evident	Evident	Invisible
4 w after modeling	Cartilage	Smooth and intact	Smooth and intact	Smooth and intact
	Cortical bone	Smooth, flat and continuous	Smooth, flat and continuous	Smooth, flat and continuous
	Chondrocyte	Normal	Normal	Normal
	Cartilage matrix	Normal	Normal	Normal
	Bone marrow hemorrhage	Invisible	Invisible	Invisible
	Edema	Invisible	Invisible	Invisible

Among rabbits in the high-intensity group and medium-intensity group, medial soft tissue injuries and intraarticular effusion were overt in the knee joints. SNRs of all groups on each MRI sequence decreased over time and there were no significant differences in SNRs among the three groups at 4 weeks. It is presumed that differences in SNR were due to distinct impact injuries induced by impact force among the three groups. As far as histopathologic variations are concerned, cartilage, cortical bone, chondrocytes, and cartilage matrix were well-aligned among all three groups at different time intervals. At 6 hours and 2 weeks, overt bone marrow hemorrhage and edema were present in the high-intensity and medium-intensity groups but they were invisible in low intensity group. According to Ghadipasha et al., visible bone marrow hemorrhage and edema were present in frozen sections extracted from the contusion regions in subchondral bone of 5 deaths from traffic accidents [19]. A study conducted by Musumeci et al. has also proven that SNRs for damaged cartilage tissue decreased gradually during rehabilitation on MRI, further validating the findings in our current study [20].

We speculate that bone marrow hemorrhage and edema induced by different impact intensities contribute to the differences in SNRs on diverse MRI sequences among the three groups. On the T1WI sequence, images were acquired with shorter TR values. During the TR

period, protons of different tissues may not reach a complete relaxation state. As a result, they cannot be fully excited by subsequent RF pulses, which further leads to decreasing echo amplitude. Consequently, SNR is low on T1WI. By contrast, T2WI provides higher resolution and allows more visible pathological changes in articular cartilage of the knee joints. It allows more favorable angiography with regards to intraarticular hemorrhage and edema of the knee joints, in determining whether defects were present at the entire cartilage plane or merely its surface. Hence, the T2WI sequence is superior to T1WI in examining SNRs. In the current study, the highest SNRs of the three groups were shown and more overt synovial fluid was visualized on GER as compared with those on conventional weighted images. Additionally, Douis et al. stated that PDWI provided excellent contrast for cartilage imaging [21]. Quasi-T2 weighted images can be created on GER using small flip angles, rendering better visualization of bone marrow hemorrhage and edema in cartilage of the knee joints. This is also consistent with the finding of a study by Lee et al. comparing hip injury imaging on MRI sequences, further verifying the results of the present study [22].

In our current study, rabbit models of impact injuries in knee joints were constructed to investigate articular cartilage injuries of the knee joint on diverse MRI sequences. However,

## Signal changes on MRI sequences and cartilage histopathologic variation

due to limited experimental conditions, findings on other MRI sequences (FID, SE) were not analyzed. Hence, additional experiments are needed for further verification.

In conclusion, there were high-signal opacities for cartilage impact injuries of knee joints on diverse MRI T1WI, T2WI, and GER sequences. High-signal opacities decreased gradually over time. On GER, signals for bone marrow hemorrhage and edema were the most evident.

### Acknowledgements

This work was supported by the Public Welfare Project of Huzhou City (A) 2016GY32.

### Disclosure of conflict of interest

None.

**Address correspondence to:** Jianyou Li, Department of Orthopedics, Huzhou Central Hospital, No. 198, Hongqi Road, Huzhou City 313003, Zhejiang Province, P.R. China. Tel: +86-13857255511; E-mail: lijianyou4902@126.com

### References

- [1] Graham J, Irving J, Tang X, Sellers S, Crisp J, Horwitz D, Muehlenbachs L, Krupnick A and Carey D. Increased traffic accident rates associated with shale gas drilling in Pennsylvania. *Accid Anal Prev* 2015; 74: 203-209.
- [2] Karimi M, Hedner J, Habel H, Nerman O and Grote L. Sleep apnea-related risk of motor vehicle accidents is reduced by continuous positive airway pressure: Swedish traffic accident registry data. *Sleep* 2015; 38: 341-349.
- [3] Kindig M, Li Z, Kent R and Subit D. Effect of intercostal muscle and costovertebral joint material properties on human ribcage stiffness and kinematics. *Comput Methods Biomech Biomed Engin* 2015; 18: 556-570.
- [4] Meran AP, Baykasoglu C, Mugan A and Toprak T. Development of a design for a crash energy management system for use in a railway passenger car. *Proceedings of the Institution of Mechanical Engineers, Part F: Journal of Rail and Rapid Transit* 2016; 230: 206-219
- [5] Kosy JD, Mandalia VI and Anaspure R. Characterization of the anatomy of the anterolateral ligament of the knee using magnetic resonance imaging. *Skeletal Radiol* 2015; 44: 1647-1653.
- [6] Sun R, Chen BC, Wang F, Wang XF and Chen JQ. Prospective randomized comparison of knee stability and joint degeneration for double- and single-bundle ACL reconstruction. *Knee Surg Sports Traumatol Arthrosc* 2015; 23: 1171-1178.
- [7] van Bussel CM, Stronks DL and Huygen FJ. Successful treatment of intractable complex regional pain syndrome type I of the knee with dorsal root ganglion stimulation: a case report. *Neuromodulation* 2015; 18: 58-60; discussion 60-51.
- [8] Grimm NL, Jacobs JC Jr, Kim J, Denney BS and Shea KG. Anterior cruciate ligament and knee injury prevention programs for soccer players: a systematic review and meta-analysis. *Am J Sports Med* 2015; 43: 2049-2056.
- [9] Collins NJ, Prinsen CA, Christensen R, Bartels EM, Terwee CB and Roos EM. Knee injury and osteoarthritis outcome score (KOOS): systematic review and meta-analysis of measurement properties. *Osteoarthritis Cartilage* 2016; 24: 1317-1329.
- [10] Whittaker JL, Woodhouse LJ, Nettel-Aguirre A and Emery CA. Outcomes associated with early post-traumatic osteoarthritis and other negative health consequences 3-10 years following knee joint injury in youth sport. *Osteoarthritis Cartilage* 2015; 23: 1122-1129.
- [11] Silverwood V, Blagojevic-Bucknall M, Jinks C, Jordan JL, Protheroe J and Jordan KP. Current evidence on risk factors for knee osteoarthritis in older adults: a systematic review and meta-analysis. *Osteoarthritis Cartilage* 2015; 23: 507-515.
- [12] Kumahashi N, Sward P, Larsson S, Lohmander LS, Frobell R and Struglics A. Type II collagen C2C epitope in human synovial fluid and serum after knee injury—associations with molecular and structural markers of injury. *Osteoarthritis Cartilage* 2015; 23: 1506-1512.
- [13] Mandl P, Navarro-Compan V, Terslev L, Aegertter P, van der Heijde D, D'Agostino MA, Baraliakos X, Pedersen SJ, Jurik AG, Naredo E, Schueller-Weidekamm C, Weber U, Wick MC, Bakker PA, Filippucci E, Conaghan PG, Rudwaleit M, Schett G, Sieper J, Tarp S, Marzo-Ortega H and Ostergaard M. EULAR recommendations for the use of imaging in the diagnosis and management of spondyloarthritis in clinical practice. *Ann Rheum Dis* 2015; 74: 1327-1339.
- [14] Yee A, Webb T, Seaman A, Infantino M, Meacci F, Manfredi M, Benucci M, Lakos G, Favalli E, Schioppo T, Meroni PL and Mahler M. Anti-CarP antibodies as promising marker to measure joint damage and disease activity in patients with rheumatoid arthritis. *Immunol Res* 2015; 61: 24-30.
- [15] Oldenburg J, Zimmermann R, Katsarou O, Theodossades G, Zanon E, Niemann B, Kellermann E and Lundin B. Controlled, cross-sectional MRI evaluation of joint status in severe

## Signal changes on MRI sequences and cartilage histopathologic variation

- haemophilia a patients treated with prophylaxis vs. on demand. *Haemophilia* 2015; 21: 171-179.
- [16] Park HJ, Lee SY, Park NH, Ahn JH, Chung EC, Kim SJ and Cha JG. Three-dimensional isotropic T2-weighted fast spin-echo (VISTA) knee MRI at 3.0 T in the evaluation of the anterior cruciate ligament injury with additional views: comparison with two-dimensional fast spin-echo T2-weighted sequences. *Acta Radiol* 2016; 57: 1372-1379.
- [17] Taneja AK, Miranda FC, Braga CA, Gill CM, Hartmann LG, Santos DC and Rosemberg LA. MRI features of the anterolateral ligament of the knee. *Skeletal Radiol* 2015; 44: 403-410.
- [18] Vavalle NA, Moreno DP, Rhyne AC, Stitzel JD and Gayzik FS. Lateral impact validation of a geometrically accurate full body finite element model for blunt injury prediction. *Ann Biomed Eng* 2013; 41: 497-512.
- [19] Ghadipasha M, Vaghefi SS, Kazemi Esfeh S, Teimoori M, Ouhadi AR and Mirhosseini SM. An annual analysis of clinical diagnosis versus autopsy findings in fatal motor vehicle accident in legal medicine organization of Kerman province, Iran. *J Forensic Leg Med* 2015; 34: 164-167.
- [20] Musumeci G, Castrogiovanni P, Leonardi R, Trovato FM, Szychlinska MA, Di Giunta A, Loreto C and Castorina S. New perspectives for articular cartilage repair treatment through tissue engineering: a contemporary review. *World J Orthop* 2014; 5: 80-88.
- [21] Douis H, Jeys L, Grimer R, Vaiyapuri S and Davies AM. Is there a role for diffusion-weighted MRI (DWI) in the diagnosis of central cartilage tumors? *Skeletal Radiol* 2015; 44: 963-969.
- [22] Lee S, Nardo L, Kumar D, Wyatt CR, Souza RB, Lynch J, McCulloch CE, Majumdar S, Lane NE and Link TM. Scoring hip osteoarthritis with MRI (SHOMRI): a whole joint osteoarthritis evaluation system. *J Magn Reson Imaging* 2015; 41: 1549-1557.